Author's Accepted Manuscript

www.elsevier.com/locate/talanta

An enzyme-free sensitive electrochemical microRNA-16 biosensor by applying a multiple signal amplification strategy based on Au/PPy–rGO nanocomposite as a substrate

Jing Bao, Changjun Hou, Yanan Zhao, Xintong Geng, Mickey Samalo, Huisi Yang, Minghong Bian, Danqun Huo

PII: S0039-9140(18)31364-X
DOI: https://doi.org/10.1016/j.talanta.2018.12.082
Reference: TAL19430

To appear in: *Talanta*

Received date: 18 September 2018
Revised date: 20 December 2018
Accepted date: 25 December 2018

Cite this article as: Jing Bao, Changjun Hou, Yanan Zhao, Xintong Geng, Mickey Samalo, Huisi Yang, Minghong Bian and Danqun Huo, An enzyme-free sensitive electrochemical microRNA-16 biosensor by applying a multiple signal amplification strategy based on Au/PPy–rGO nanocomposite as a substrate, *Talanta,* https://doi.org/10.1016/j.talanta.2018.12.082

An enzyme-free sensitive electrochemical microRNA-16 biosensor by applying a multiple signal amplification strategy based on Au/PPy–rGO nanocomposite as a substrate

Jing Bao[a], Changjun Hou[a]*, Yanan Zhao[a], Xintong Geng[a], Mickey Samalo[a], Huisi Yang[a], Minghong Bian[b], Danqun Huo[b]*

[a]Key Laboratory of Biorheological Science and Technology (Chongqing University), Ministry of Education, College of Bioengineering, Chongqing University, Chongqing 400044, PR China

[b]Liquor Making Biology Technology and Application of Key Laboratory of Sichuan Province, College of Bioengineering, Sichuan University of Science and Engineering, Zigong, 643000, PR China

houcj@cqu.edu.cn

huodq23@163.com

*Corresponding authors. Tel.: +86 23 6511 2673; fax: +86 23 6510 2507.

Abstract

In present study, a sensitive and effective electrochemical microRNA (miRNA) sensing platform is successfully developed by integrating gold nanoparticles /polypyrrole-reduced graphene oxide (Au/PPy-rGO), catalyzed hairpin assembly (CHA) and hybridization chain reaction (HCR) multiple signal amplification strategy. Firstly, Au/PPy–rGO was employed onto a bare GCE by electrodeposition that can greatly enhanced conductivity and effectively immobilize probes. Then, the thiolated capture probes (SH-CP) were self-assembled on the Au/PPy–rGO modified GCE via

Au-S bond. The target miRNA triggered the dynamic assembly of the two hairpin substrates (H1 and H2), leading to the cyclicality of the target miRNA and the formation of H1–H2 complexes without the assistance of enzyme. Subsequently, the newly emerging DNA fragment of H2 triggered the HCR when a mixture solution (hairpins H3 and H4) and produced dsDNA polymers. Finally, a substantial amount of methylene blue (MB) as signal indicator was intercalated into the minor groove of the long dsDNA polymers to achieve detected electrochemical signal. The fabricated sensor is able to detect miRNA-16 (model target) with concentration range from 10 fM to 5 nM with a low detection limit (LOD) of 1.57 fM (S/N=3). Current research suggests that the developed multiple signal amplification platform has a great potential for the applications in the field of biomedical research and clinical analysis.

Graphical Abstract

An enzyme-free sensitive electrochemical microRNA-16 biosensor was constructed by integrating gold nanoparticles/polypyrrole-reduced graphene oxide nanocomposite (Au/PPy-rGO), catalyzed hairpin assembly (CHA), and hybridization chain reaction (HCR) multiple signal amplification strategy, and it exhibited excellent sensing performance for miRNA-16 reduction with large linear concentration range and low detection limit.

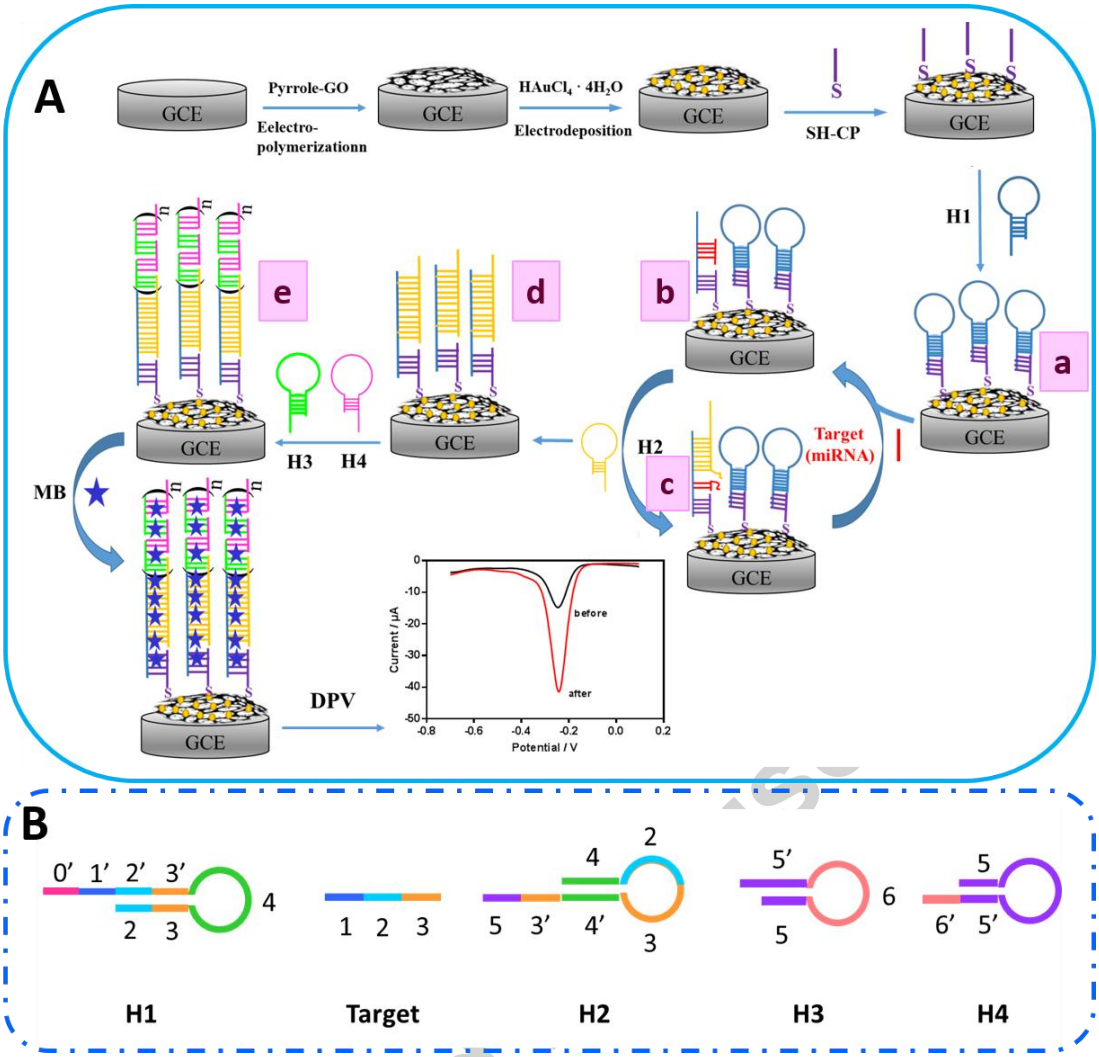

Keywords: MicroRNA, Enzyme-free detection, Multiple signal amplification, Electrochemical sensing.

1. Introduction

MicroRNAs (miRNAs), a family of endogenous small and non-coding RNAs with 18-25 nucleotides (nts), play a critical role in gene expression and biological processes, for instance, cellular development, proliferation, differentiation, metabolism, and tumorigenesis etc [1-3]. Recently, some clinical studies demonstrated that the alteration expression levels of many miRNAs remarkably alter the associated with tumor progression, thus it has become novel diagnostic markers for cancer diagnosis, therapy, and prognosis [4-8]. Many studies identified that miRNA-16 family members could serve as biomarkers in the diagnosis of the related diseases, including Gastric cancer (GC) [9], diffuse large B cell lymphoma (DLBCL) [10], oral cancer [11], nasopharyngeal cancer [12] and breast cancer [13], and it could distinguish cancer patients from non-cancer people [14]. Therefore, miRNA-16 was chosen as the target miRNA in the detection.

On account of the correlation between miRNAs and human serious diseases, it's important to develop convenient, rapid, efficient, reliable, ingenious approach for the detection of miRNAs. However, the intrinsic characteristics of miRNA, such as short sequence, low abundance, vulnerable degradability, high sequence similarity among their family members, and relatively low expression levels, make it extremely hard to be detected in real samples [15]. Conventional methods for miRNA detection such as northern blot analysis [16-17], molecular cloning [18-19], polymerase chain reaction (PCR) [20-21], microarray assay [22-23], suffer the limitations that hindered their applications in clinical diagnostic, such as poor sensitivity, time-consuming, low throughput, complex data analysis , requirement of sophisticated instrumentation and skilled professionals, which limited their widespread applications in clinical diagnostics. To surmount these shortcomings, extensive methods using different signal readout assays have been developed recently, such as surface plasmon resonance (SPR) [24], colorimetric measurement [25], fluorescence [26], electrochemiluminescence (ECL) [27] and electrochemical biosensor [28-29]. Among them, electrochemical biosensors for the quantification of miRNA are currently gaining an increasing attention due to its many significant advantages, for instance, high sensitivity and selectivity, relatively low cost, fast response, portability, and simple operation [30].

In order to further enhance the sensitivity of electrochemical biosensors, a

number of signal amplification techniques have been widely developed, such as hybridization chain reaction (HCR) [31], catalyzed hairpin assembly (CHA) [32], rolling circle amplification (RCA) [33-34], nuclease amplification [35] and nanomaterials based techniques [36-37]. CHA strategy has attracted keen interest in miRNA detection because of its enzyme-free peculiarity and the target miRNA can be cyclically utilized for many times to amplify electrochemical signal even though the level of target miRNA in the sample is low [38]. HCR amplification can bind thousands of auxiliary hairpin probes and produces long nicked double-strands (dsDNA) molecule without the assistance of enzyme, which is relatively convenient in sensing field [39-40]. Most recently, nanomaterials (AuNPs and carbon materials, etc.) were popularly employed as electrode supporting substrates to achieve signal amplification in miRNA detection due to their excellent conductivity, high specific surface area to volume ratio, good biocompatibility, and size-dependent properties [41]. Based on previous study, reduced graphene oxide (rGO) was co-deposited with pyrrole (Py) through electrochemical cyclic voltammetry to form a homogeneous membrane (PPy–rGO) on the surface of the electrode. The rGO was especially incorporated into the polypyrrole (PPy) to avoid aggregation owing to strong chemisorptions between carbon materials and polymers, and it also provides several functional groups such as carboxyl (-COOH) and hydroxyl (-OH) groups resulting in the higher conductivity, which is beneficial to the growth of metal nanoparticles in the fabrication of nanocomposites [42-44]. Finally, AuNPs were electrodeposited on the PPy–rGO surface to form Au/PPy–rGO nanocomposite in this work, providing a large surface area and conductive platform for the immobilization of probes.

Herein, using miRNA-16 as a model target, we integrated nanocomposite (Au/PPy–rGO), CHA and HCR signal amplification strategies to fabricate a multiple signal amplification electrochemical biosensors for sensitive detection of miRNA. Au/PPy–rGO nanocomposite was employed as support substrate to amplify the electrochemical signal, increasing the sensitivity of fabricated miRNA biosensor enormously. Then, capture probes (SH-CP) were self-assembled onto Au/PPy–rGO modified GCE via Au-S bond. Hairpins (H1 and H2) were triggered by the target miRNA (miRNA-16) to form a double helix structure, realizing the CHA reaction which led to the cyclicality of the target miRNA. The exposed DNA fragment of H2 then served as a trigger to induce the hybridization reaction (HCR), yielding a long dsDNA molecule until the hairpins of H3 or H4 is exhausted. Finally, a substantial

amount of methylene blue (MB) as redox probes could be intercalated into the double-stranded DNA (dsDNA) through π-π stacking interactions to achieve detected electrochemical signal. The proposed platform provides a general and promising strategy for ultrasensitive detection of miRNAs in clinical diagnosis.

2. Experiments

2.1 Reagents and materials

Pyrrole (98%), hydrogen tetrachloroaurate trihydrate ($HAuCl_4 \cdot 3H_2O$), sodium dodecylbenzenesulfonate (SDBS), dodecylbenzene sulfonic acid (DBSA, >99%), disodium ethylenediamine tetraacetic acid (EDTA) and tri (2-carboxyethyl) phosphine hydrochloride (TCEP) were purchased from Aladdin (Shanghai, China). Tris–HCl and methylene blue (MB) were obtained from Sigma-Aldrich (St. Louis, USA) and used as received. 6-mercapto-1-hexanol (MCH) was purchased from Adamas Reagent Co., Ltd. (Shanghai, China). 20 bp DNA ladder, DL 500 DNA marker, and 10×Loading buffer were purchased from TaKaRa Biotechnology Co., Ltd (Dalian, China). Agarose was provided by Invitrogen Biotechnology Co., Ltd (Carlsbad, CA, USA). The normal human sera were purchased from Solarbio Tech Co., Ltd. (Beijing, China).

HPLC-purified oligonucleotide sequences were designed according to previously reported methods. The oligonucleotides were synthesized and purified from Sangon Biotechnology Co. (Shanghai, China). The base sequences were summarized in Table 1. The buffer solutions employed in this work were purchased from Sangon Biotechnology Co. (Shanghai, China). All other chemicals were analytical-reagent grade and were used as received. All aqueous solutions were freshly prepared with deionized distilled (DI) water (18.2 MΩ·cm) with a Millipore system.

2.2 Apparatus and electrochemical measurements

The prepared electrodes were morphologically characterized by FEI Nova 400 field-emission scanning electron microscope (FESEM), energy dispersive spectroscopy (EDS) and X-ray diffraction (XRD) measurements. Electrophoresis apparatus DYY-6C was employed in electrophoresis experiments and the gel image was recorded on an azure biosystems cSeries imaging systems. All electrochemical measurements were carried out using a CHI 760E electrochemical workstation (Shanghai Chenhua Instruments Co. Ltd, China) with a conventional three-electrode system inculuding a modified GCE (GCE, Φ = 3 mm), a platinum wire (counter electrode) and a silver/silver chloride (Ag/AgCl) reference electrode. All the measurements were triplicated and obtained at room temperature.

2.3 Gel electrophoresis

Electrophoresis analysis were carried out on 3.5% agarose gel and ran at a constant voltage at 80 V for 35 min in 0.5 × tris-borate-EDTA buffer (TBE, pH 8.0) at room temperature. Then, the nucleic acid dye was Nucleic Acid Red (NA-Red). Samples for agarose gel electrophoresis assays were prepared as follows: (1) 20 bp DNA ladder, (2) H1, (3) H2, (4) H1+H2, (5) H1+T+H2, (6) H1+T+H2/H3+H4; T: target miRNA (miRNA-16). The concentration of each sample in agarose gel was 3 μM.

2.4 Synthesis of rGO and electrochemical polymerization of AuNPs/PPy-rGO

Graphene oxide (GO) was synthesized from natural graphite powder according to a classical Hummer's method with modification [45]. 0.01 M SDBS was added to 100 mL aqueous suspension of GO at a concentration of 0.1 mg mL^{-1} under ultrasonic treatment for 2 h. Then, the color of the above solution changed to black after SDBS-modified GO was reduced with hydrazine (30 mL) and heated at 100 °C for over 24 h [46]. The obtained rGO–SDBS was centrifuged out, washed with DI water for several times, and dried in vacuum environment overnight.

Prior to the electrode modification, the bare GCE was polished with 0.3 and 0.05 μm alumina slurries, then sonicated in acetone, ethanol and DI water for 30 s. After that, the GCE was immersed into a deposition solution containing 0.1 M pyrrole, 1 mg ml^{-1} rGO–SDBS, 0.02 M DBSA and protected with N_2. The PPy-rGO was deposited by CV from -0.2 to 1.2 V for 8 cycles and intensive washed with PBS buffer. In addition, the gold nanoparticles (Au) were further deposited onto the PPy-rGO/GCE in 0.1% $HAuCl_4$ solution containing 0.01 M H_2SO_4 and Na_2SO_4 (v/v=1:1) at the potential of -0.2 V for 300 s to obtain Au/PPy-rGO/GCE [47].

2.5 Fabrication of the proposed biosensor

Prior to use, all the hairpin oligonucleotides were annealed at 95 °C for 5 min, then were slowly cooled at room temperature [48]. A 20 μL aliquot of SH-CP (5 μM) solution was freshly reacted with 10 μL of 10 mM TCEP solution for 1 h at room temperature to reduce the disulfide bonds. The schematic diagram of the stepwise fabrication procedure was illustrated in Scheme 1A. First of all, a droplet of 5μL of 5 μM SH-CP solution was directly cast onto the surface of AuNPs/PPy-rGO/GCE and incubated for 2 h at 37°C condition via Au-S bonding. The modified electrode was rinsed three times with PBS, the resulting electrode surface was blocked with 2 mM

MCH solution for 1 h and rinsed with distilled water. Subsequently, 10 μL mixture solution (H1 and H2) with different concentrations of the target (miRNA-16) was dropped on the modified GCE and incubated for 2 h at 37 °C to trigger the CHA, followed by a thorough washing with PBS and DI water. Then, the modified electrode was immersed in 20 μL mixture containing 1 μM H3 and 1 μM H4 at 37 °C for 2 h (HCR) and terminated by thorough washing. The as-prepared electrode was immersed into 1 mM MB for 30 min, resulting in the accumulation of MB into the double-stranded DNA (dsDNA) polymers by a non-covalent manner, which served as an electron mediator to give the electrochemical signal for miRNA detection [49-50].

3. Results and discussion

3.1 Mechanism of the proposed miRNA biosensor

Scheme 1A illustrated the principle of multiple signal amplification-based biosensor for the detection of miRNA, and involved three main stages: (1) AuNPs/PPy-rGO was used as support substrate to immobilize SH-CP through Au–S binding; (2) a double helix structure of H1-H2 was formed by a catalyzed hairpin assembly reaction (CHA); (3) the formation of longer DNA strands through the hybridization chain reaction (HCR). According to earlier approaches [51-54], we designed hairpin probes (H1, H2, H3 and H4) containing an occluding complementary domain within the intramolecular hairpin secondary structure, respectively (Scheme 1B and Fig. S1). Two stable hairpin species did not originally interact but could catalytically form a stable duplex in the presence of target oligonucleotide sequence [51, 55]. Hairpins H1 and H2 were composed of five (0', 1', 2, 3, 4) and four (2, 3, 4, 5) numbered domains, respectively, and each of numbered domain represents a short fragment sequence. Complementarity to the corresponding domain is denoted by a prime symbol (') with the same numbered domain. The stem-loops with bulky structures significantly reduced the surface density at the Au/PPy-rGO, therefore, we used domain 0' of H1 as a linker to hybridize with SH-CP (0) to increase the surface density without conformational change (Scheme 1A, a) [56-57]. Domain 1-2-3 of target miRNA, (T), serves as a 'toehold region' to initiate a branch migration with stem of H1 (Domain 1'-2'-3'). The introduction of target miRNA (T) could open the hairpin structure of H1 and hybridize it to form H1-T intermediate x by strand-displacement reaction (Scheme 1A, b). The newly emerging domain 3' of H1-T intermediate initiates a branch migration reaction to form an unstable H1-H2-T complex (Scheme 1A, c). After a stable H1/H2 duplex were

conformed (Scheme 1A, d) the target miRNA were simultaneously liberated, resulting to the cyclicality of the target miRNA (T) and the CHA products. When the mixture (H3 and H4) was added, the newly exposed toehold 5 of H2 served as trigger to induce hybrid chain reaction (HCR), aiming to in situ form a steady stream dsDNA copolymers until the supply of H3 or H4 is exhausted (Scheme 1A, e) [58]. Ultimately, a large amount of MB was intercalated into the minor groove of the long dsDNA polymers to response electrochemical signal for the detection of miRNA [49].

3.2 Characterization of the Au/PPy-rGO nanocomposite

The morphologies of the prepared samples were characterized by SEM (Fig.1). The as-prepared electrochemically polymerized polypyrrole (PPy) presents compact and a typical cauliflower architecture (Fig. 1A). When mixing reduced graphene oxide (rGO) with pyrrole in deposition solution, the PPy–rGO nanocomposite was electropolymerized onto the surface of electrode. Fig. 1B displays the top view of the PPy–rGO nanocomposite with a flexible and crumpled paper-like film, which was clearly distinguished from PPy. The AuNPs with a diameter of ~30 nm were uniformly deposited on the both layers and skeleton of the PPy–rGO nanocomposite (Fig. 1C), suggesting efficient and successful electrodeposition of AuNPs into PPy–rGO. Furthermore, the prepared Au/PPy–rGO nanocomposite, with an increased surface roughness and excellent electric conductivity, was used as substrate to immobilize SH-CP and also facilitate electron transfer of the biosensor. To further confirm the successful synthesize of Au/PPy–rGO, EDS element mapping analysis and X-ray diffraction (XRD) measurements were carried out. The synthesized nanocomposite contains C, N, O and Au elements and all elements are uniformly distributed throughout the whole selected Au/PPy–rGO (Fig. 1D). As shown in Fig. S2, the diffraction peaks located at 2θ values of 38.65°, 44.6°, 64.6°, 77.7° and 82.4° are assigned to (111), (200), (220), (311) and (222) planes of Au, respectively, while a diffraction peak located at 2θ value of 25.7° is corresponding to (002) plane of C (PPy–rGO), implying the successful synthesize of Au/PPy–rGO composite.

3.3 Electrochemical characterization of the proposed miRNA biosensor

The stepwise process of the working electrode was systematacially investigated by CV and EIS in 5 mM $[Fe(CN)_6]^{3-/4-}$ (1:1) solution containing 0.1 M KCl from -0.2 V to +0.6 V. As shown in Fig.2A, a pair of well-defined quasi-reversible redox peaks

of $[Fe(CN)_6]^{3-/4-}$ were obtained at the bare GCE (Fig.2A, curve a). When Au/PPy–rGO nanocomposite was electrodeposited on the GCE surface, the redox peak currents obviously increased (Fig.3A, curve b) owing to the excellent conductivity of Au/PPy–rGO and the enhanced effective surface area of the electrode, which could significantly accelerate the electron transfer. In contrast, the current response was reduced dramatically when capture probes (SH-CP) were immobilized through Au-S bond (Fig.2A, curve c), which can be explained as the fact that SH-CP can hinder the electron transfer rate between the electrode and $[Fe(CN)_6]^{3-/4-}$. After the mixture solution (H1, miRNA-16 and H2) were added and double helix structures of H1-H2 were formed by a catalyzed hairpin assembly reaction (CHA), a dramatic decrease in redox current peaks were noted (Fig.2A, curve d). This phenomenon occurred because the polymerization of dsDNA on the surface of the electrode increased the electrostatic repulsion between the negatively charged DNA backbone and $[Fe(CN)_6]^{3-/4-}$. As expected, the peak current further decreased when a mixture (H3 and H4) was added (Fig.2A, curve e). It confirmed the occurrence of hybridization chain reaction (HCR) and the formation of longer DNA strands on the electrode surface could further repel the diffusion of ferricyanide toward the electrode surface.

EIS is an effective and convenient method for investigating the charge transfer properties of the stepwise modified electrode. As illustrates in the inset of Fig. 2B, a Randles equivalent electrical circuit is employed to fit all the electrical parameters of the EIS. In these circuits, R_s is primarily the resistance of the electrolyte solution; R_{ct} is the charge transfer resistance; Z_w is the Warburg impedance related to the diffusion of ions in the bulk electrode; C is capacity of the double layer [59]. First, the bare GCE exhibited the R_{ct} of approximately 615 Ω (Fig. 2B, curve a) with a small semicircle. After Au/PPy–rGO was electrodeposited on GCE, the R_{ct} decreased significantly and displayed an almost straight line (Fig. 2B, curve b) due to the excellent conductivity of the composite. Then, the R_{ct} greatly increased to about 1155 Ω (Fig. 2B, curve c) when the SH-CP was assembled onto the electrode surface, demonstrating that capture probes were successfully combined on the Au/PPy–rGO/GCE via Au-S bond. As expected, a further increased R_{ct} value (1825 Ω) was observed as a result of the negatively charged phosphoric acid backbones of dsDNA (H1-H2) immobilized on the electrode surface (Fig. 2B curve d). With the addition of locked hairpins H3 and H4 mixtures, the value of R_{ct} increased to 3688 Ω (Fig. 2B curve e), which could be interpreted as the successful HCR process and the fact that

more negatively charged dsDNA polymers were linked on the modified electrode. All of the EIS results were identical with the changes observed in CV, which confirmed the successful fabrication of the miRNA biosensor.

3.4 Signal amplification properties of CHA and HCR

At first, the process of CHA and HCR were verified using target miRNA with agarose gel electrophoresis. As seen in Fig. S3, hairpin DNA segments (H1 (lane 2) and H2 (lane 3)) could not hybridize with each other in absence of target miRNA (lane 4), only maintaining the hairpin stem region with each other. However, hybridization of H1 and H2 was initiated in the presence of target miRNA (T), resulting a newly bright band (lane 5). When the locked hairpins (H3 and H4) were added, HCR was triggered by the newly emerging DNA fragment of H2, resulting in many longer dsDNA polymers (lane 6). The electrophoresis results implied that the introduction of target miRNA (T) could open the hairpin structure of H1 and trigger CHA, and the occurrence of HCR could produce long dsDNA molecule.

The signal amplification properties of the proposed approach were also investigated using DPV method toward the as-prepared electrodes in 0.1 M PBS (pH=7.4). Fig. 3 displays a feeble peak current when only SH-CP and H1 were assembled onto the electrode surface (Fig. 3, curve a). After the addition of only H2, the current change between curve a and b was nearly negligible (Fig. 3, curve b), which demonstrated that the H2 failed to immobilize on H1/SH-CP/Au/PPy-rGO/GCE. The reason of this phenomena was that two stable hairpins could coexist in solution [60]. By contrast, after simultaneously adding target miRNA-16 (5 nM) and H2, a distinct increase in current signal was obtained (Fig. 3, curve c) due to the occurrence of CHA to form a stable H1/H2 duplex. Furthermore, the peak current signal was dramatically increased when the electrode was immersed in locked hairpins H3 and H4 mixtures (Fig. 3, curve d). This phenomenon attributed the successful HCR process to gain longer dsDNA molecule and more accumulation amounts of MB to gain higher current signal.

3.5 Optimization of the experimental conditions

To achieve higher analytical performance of the developed miRNA biosensor, the concentration of H2 and the incubation time of CHA were selectively optimized and the corresponding results are showed in Fig. 4. As shown in Fig. 4A, with the addition of different concentrations of H2 from 0.6 μM to 1.4 μM in mixture (1 μM H1 and 5 nM target miRNA), the peak current of MB increased sharply up to 1.2 μM

and then gradually leveled off. Therefore, 1.2 μM were chosen as the optimal concentration of H2. The effect of the incubation time of CHA, which was related to the density of the double helix structure of H1-H2 on the electrode were also tested. The incubation time of CHA on the DPV response was optimized in the range of 30–150 min without other condition changes. With the prolongation of incubation time, the peak current of MB initially increases almost linearly within 120 min and remained stable thereafter (Fig. 4B), indicating that the reaction equilibrium was reached. Thus, 120 min was selected as the optimal incubation time of CHA in subsequent experiments.

3.6 Analytical performance of the proposed miRNA biosensor

The analytical performance of the developed biosensor in miRNA-16 detection with different concentrations was investigated by DPV measurements under the optimal conditions (Fig.5). The DPV responses of MB linearly increased with the logarithm of miRNA-16 concentrations in the range of 10 fM ~ 5 nM (Fig. 5A). The corresponding regression equation can be expressed as $I(\mu A) = -5.91227 \log c - 87.833$ with a coefficient of determination (R^2) of 0.99353, where c represents concentrations of miRNA-16 (n=3) (Fig. 5B). The limit of detection (LOD) was calculated to be ~1.57 fM (S/N=3). More comparisons of this work with reported in earlier studies on miRNA detection were shown in Table S1. The good sensing performance can be attributed to the synergistic effect of two factors: (1) Au/PPy–rGO nanohybrid with high specific surface area and good conductivity provided more effective electroactive sites to immobilize on electrode that enhanced the performance of biosensor; (2) the combination of signal amplifications of CHA and HCR to amplify the signal readout and improve the detection sensitivity of biosensor.

3.7 Specificity, reproducibility and stability of the proposed miRNA biosensor

The selectivity of the developed biosensor was verified by exposing it to four types of sequences including perfect complementary sequence, single-base mismatch (sRNA) sequence, non-complementary DNA (nDNA) sequence, and non-complementary RNA (nRNA) sequence (miRNA-155) under identical conditions. As expected shown in Fig. 6, the proposed biosensor exhibited negligible interference to 500 pM sRNA (b), 500 pM nDNA (c) and 500 pM nRNA (d), and the results were nearly the blank ground current (a). Interestingly, the current variation of perfect complementary strand, 500 pM target miRNA-16 (e), was nearly 6-fold than that of

central mismatched sequences. These current responses demonstrated that the proposed miRNA sensing strategy showed a high electrochemical specificity toward the target miRNA.

Assay stability was evaluated by 30-continuous cycles CV measurements in 0.1 M pH 7.4 PBS with the range from -0.7 to 0.2 V after incubating 500 pM miRNA-16 (Fig. S4) and a relative standard 4.55% were acquired. Long-term stability of the fabricated biosensor was further tested and the biosensor could Rctain about 93.6% of its initial stable response value after two-week storage at 4 °C (Fig. S5). Reproducibility of the proposed biosensor was also investigated. Five modified electrodes prepared with the same procedure were incubated with 500 pM miRNA-16. All electrodes showed similar signals and a relative standard deviation (RSD) of 4.37% was acquired. Generally speaking, these results suggested that the biosensor for detecting miRNA-16 possessed satisfactory stability and acceptable reproducibility.

3.8 Analytical application of the miRNA biosensor

To monitor the practical applicability of the prepared biosensor, recovery experiments were performed through the standard addition method by adding different concentrations (0.5, 1, 50 and 100 pM) of miRNA-16 into the 10-fold diluted blank human serum samples. As summarized in Table S2, the calculated recovery in real serum samples were observed in the range from 92.68% to 105.7% with the RSD values ranging from 2.13% to 6.37%, respectively. This finding demonstrated that the proposed strategy showed good potential as a practical tool to monitor miRNA in real biological samples.

Conclusion

In the present work, we successfully developed an ultrasensitive electrochemical biosensor for amplified miRNA-16 detection through multiple signal amplifications. Several advantages of the fabricated biosensor should be highlighted: (1) the synthesized nanocomposite of Au/PPy–rGO increased the surface area and also showed excellent conductivity, thus enhancing the electron transfer; (2) The combination of CHA and HCR accomplished the target recycling and signal amplification without the assistance of protein enzymes; (3) With the above signal amplification strategies, the fabricated miRNA biosensor displayed not only a sensitive detection limit of 1.57 fM (miRNA-16) and a wider linear range of 10 fM ~

5 nM but also high selectivity, satisfactory stability and ideal reproducibility; (4) The proposed multiple signal amplification strategy could be conveniently extended to detect other cancer related miRNAs by simply altering the corresponding sequence. In summary, the proposed approach is a valuable platform for sensitive detection of miRNA, suggesting a promising potential in early cancer prevention and detection.

Acknowledgements

This work was supported by the National Natural Science Foundation of China (NO. 81772290 and 81271930), Graduate research and innovation foundation of Chongqing, China (CYB17037), Chongqing University innovation training program for College Students (201710611100), Chongqing science and technology commission (CSTC2015shmszxl20097), the workstation in Sichuan Province GY2015-01 and sharing fund of Chongqing university's large equipment.

References:

[1] L. Ma, J. Zhao, T. Li, Y. He, J. Wang, L. Xie, X. Qin and S. Li, Association between Tumor necrosis factor-alpha gene polymorphisms and prostate cancer risk: a meta-analysis, Diagn. Pathol. 74 (2014).

[2] T. Kilic, A. Erdem, M. Ozsoz and S. Carrara, microRNA biosensors: Opportunities and challenges among conventional and commercially available techniques, Biosens. Bioelectron. (2018) 525-546.

[3] P. Miao, F. Meng, B. Wang, X. Zhu and Y. Tang, Highly sensitive microRNA quantification with zero background signal from silver nanoparticles, Electrochem. Commun. (2015) 89-92.

[4] R.M. Torrente-Rodriguez, S. Campuzano, V. Ruiz-Valdepenas Montiel, J.J. Montoya and J.M. Pingarron, Sensitive electrochemical determination of miRNAs based on a sandwich assay onto magnetic microcarriers and hybridization chain reaction amplification, Biosens. Bioelectron. (2016) 516-521.

[5] H. Dong, J. Lei, L. Ding, Y. Wen, H. Ju and X. Zhang, MicroRNA: Function, Detection, and Bioanalysis, Chem. Rev. 8 (2013) 6207-6233.

[6] P. Mestdagh, N. Hartmann, L. Baeriswy, D. Andreasen, N. Bernard, C. Chen, D. Cheo, P. D'Andrade, M. DeMayo, L. Dennis, S. Derveaux, Y. Feng, S. Fulmer-Smentek, B. Gerstmayer, J. Gouffon, C. Grimley, E. Lader, K.Y. Lee, S. Luo, P. Mouritzen, A. Narayanan, S. Patel, S. Peiffer, S. Ruberg, G. Schroth, D. Schuster, J.M. Shaffer, E.J. Shelton, S. Silveria, U. Ulmanella, V. Veeramachaneni, F. Staedtler, T. Peters, T. Guettouche and J. Vandesompele, Evaluation of quantitative miRNA expression platforms in the microRNA quality control (miRQC) study, Nat. Method. 8 (2014) 809-815.

[7] J. Zhang, L. Wang, M. Hou, Y. Xia, W. He, A. Yan, Y. Weng, L. Zeng and J. Chen, A ratiometric electrochemical biosensor for the exosomal microRNAs detection based on bipedal DNA walkers propelled by locked nucleic acid modified toehold mediate strand displacement reaction, Biosens.

Bioelectron. (2018) 33-40.

[8] Y. Yuan, S. Chi, S. Wen, R. Liang, Z. Li and J. Qiu, Ratiometric electrochemical assay for sensitive detecting microRNA based on dual-amplification mechanism of duplex-specific nuclease and hybridization chain reaction, Biosens. Bioelectron. (2018) 211-216.

[9] H. Wang, L. Wang, Z. Wu, R. Sun, H. Jin, J. Ma, L. Liu, R. Ling, J. Yi, L. Wang, J. Bian, J. Chen, N. Li, S. Yuan and J. Yun, Three dysregulated microRNAs in serum as novel biomarkers for gastric cancer screening, Med. Oncol. 29812 (2014) .

[10] C. Fang, D. Zhu, H. Dong, Z. Zhou, Y. Wang, L. Liu, L. Fan, K. Miao, P. Liu, W. Xu and J. Li, Serum microRNAs are promising novel biomarkers for diffuse large B cell lymphoma, Ann. Hematol. 4 (2012) 553-559.

[11] S.A. MacLellan, J. Lawson, J. Baik, M. Guillaud, C.F. Poh and C. Garnis, Differential expression of miRNAs in the serum of patients with high-risk oral lesions, Cancer. Med-us. 2 (2012) 268-274.

[12] X. Liu, H. Luo, W. Tian, J. Lu, G. Li, L. Wang, B. Zhang, B. Liang, X. Peng, S. Lin, Y. Peng and X. Li, Diagnostic and prognostic value of plasma microRNA deregulation in nasopharyngeal carcinoma, Cancer Biol. Ther. 12 (2013) 1133-1142.

[13] N. Mobarra, A. Shafiee, S.M.A.H. Rad, N. Tasharrofi, M. Soufi-zomorod, M. Hafizi, M. Movahed, F. Kouhkan and M. Soleimani, Overexpression of microRNA-16 declines cellular growth, proliferation and induces apoptosis in human breast cancer cells, In. Vitro. Cell. Dev-an. 6 (2015) 604-611.

[14] J. Cui, MiR-16 family as potential diagnostic biomarkers for cancer: a systematic review and meta-analysis, Int. J. Clin. Exp. Med. 2 (2015) 1703-1714.

[15] Y. Zhao, F. Chen, Q. Li, L. Wang and C. Fan, Isothermal Amplification of Nucleic Acids, Chem. Rev. 22 (2015) 12491-12545.

[16] E. Berezikov, E. Cuppen and R.H.A. Plasterk, Approaches to microRNA discovery, NAT GENET (2006) S2-S7.

[17] G.S. Pall, C. Codony-Servat, J. Byrne, L. Ritchie and A. Hamilton, Carbodiimide-mediated cross-linking of RNA to nylon membranes improves the detection of siRNA, miRNA and piRNA by northern blot, Nucleic. Acids. Res e608 (2007) .

[18] M.D. Mattie, C.C. Benz, J. Bowers, K. Sensinger, L. Wong, G.K. Scott, V. Fedele, D. Ginzinger, R. Getts and C. Haqq, Optimized high-throughput microRNA expression profiling provides novel biomarker assessment of clinical prostate and breast cancer biopsies, Mol. Cancer. 24 (2006) .

[19] M. Lagos-Quintana, R. Rauhut, W. Lendeckel and T. Tuschl, Identification of novel genes coding for small expressed RNAs, Science 5543 (2001) 853-858.

[20] C.F. Chen, D.A. Ridzon, A.J. Broomer, Z.H. Zhou, D.H. Lee, J.T. Nguyen, M. Barbisin, N.L. Xu, V.R. Mahuvakar, M.R. Andersen, K.Q. Lao, K.J. Livak and K.J. Guegler, Real-time quantification of microRNAs by stem-loop RT-PCR, Nucleic. Acids. Res. e17920 (2005) .

[21] T.D. Schmittgen, J.M. Jiang, Q. Liu and L.Q. Yang, A high-throughput method to monitor the expression of microRNA precursors, Nucleic. Acids. Res. e434 (2004) .

[22] E. Clancy, M. Burke, V. Arabkari, T. Barry, H. Kelly, R.M. Dwyer, M.J. Kerin and T.J. Smith, Amplification-free detection of microRNAs via a rapid microarray-based sandwich assay, Anal. Bioanal. Chem. 14 (2017) 3497-3505.

[23] J.M. Thomson, J. Parker, C.M. Perou and S.M. Hammond, A custom microarray platform for analysis of microRNA gene expression, Nat. Methods. 1 (2004) 47-53.

[24] S. Fang, H.J. Lee, A.W. Wark and R.M. Corn, Attomole microarray detection of MicroRNAs by nanoparticle-amplified SPR imaging measurements of surface polyadenylation reactions, J. Am. Chem.

Soc. 43 (2006) 14044-14046.

[25] R. Li, B. Yin and B. Ye, Ultrasensitive, colorimetric detection of microRNAs based on isothermal exponential amplification reaction-assisted gold nanoparticle amplification, Biosens. Bioelectron. (2016) 1011-1016.

[26] L. Yang, C. Liu, W. Ren and Z. Li, Graphene Surface-Anchored Fluorescence Sensor for Sensitive Detection of MicroRNA Coupled with Enzyme-Free Signal Amplification of Hybridization Chain Reaction, ACS Appl. Mater. Inter. 12 (2012) 6450-6453.

[27] L. Peng, P. Zhang, Y. Chai and R. Yuan, Bi-directional DNA Walking Machine and Its Application in an Enzyme-Free Electrochemiluminescence Biosensor for Sensitive Detection of MicroRNAs, Anal. Chem. 9 (2017) 5036-5042.

[28] Y. Tao, D. Yin, M. Jin, J. Fang, T. Dai, Y. Li, Y. Li, Q. Pu and G. Xie, Double-loop hairpin probe and doxorubicin-loaded gold nanoparticles for the ultrasensitive electrochemical sensing of microRNA, Biosens. Bioelectron. (2017) 99-105.

[29] H. McArdle, E. Spain, T.E. Keyes, R.L. Stallings, M. Brennan-Fournet and R.J. Forster, Triangular silver nanoplates: Properties and ultrasensitive detection of miRNA, Electrochem. Commun. (2017) 23-27.

[30] W. Cai, S. Xie, Y. Tang, Y. Chai, R. Yuan and J. Zhang, A label-free electrochemical biosensor for microRNA detection based on catalytic hairpin assembly and in situ formation of molybdophosphate, Talanta (2017) 65-71.

[31] L. Liu, C. Song, Z. Zhang, J. Yang, L. Zhou, X. Zhang and G. Xie, Ultrasensitive electrochemical detection of microRNA-21 combining layered nanostructure of oxidized single-walled carbon nanotubes and nanodiamonds by hybridization chain reaction, Biosens. Bioelectron. (2015) 351-357.

[32] R. Liu, Q. Wang, Q. Li, X. Yang, K. Wang and W. Nie, Surface plasmon resonance biosensor for sensitive detection of microRNA and cancer cell using multiple signal amplification strategy, Biosens. Bioelectron. (2017) 433-438.

[33] R.M. Dirks and N.A. Pierce, Triggered amplification by hybridization chain reaction, P. Natl. Acad. Sci. USA 43 (2004) 15275-15278.

[34] D. Han, C. Wu, M. You, T. Zhang, S. Wan, T. Chen, L. Qiu, Z. Zheng, H. Liang and W. Tan, A cascade reaction network mimicking the basic functional steps of adaptive immune response, Nat. Chem. 10 (2015) 836-842.

[35] P. Miao, Y. Tang, Q. Zhang, B. Bo and J. Wang, Identification of Cellular MicroRNA Coupling Strand Displacement Polymerization and Nicking-Endonuclease-Based Cleavage, Chempluschem. 12 (2015) 1712-1715.

[36] H. Shuai, K. Huang, Y. Chen, L. Fang and M. Jia, Au nanoparticles/hollow molybdenum disulfide microcubes based biosensor for microRNA-21 detection coupled with duplex-specific nuclease and enzyme signal amplification, Biosens. Bioelectron. 2 (2017) 989-997.

[37] X. Wu, Y. Chai, P. Zhang and R. Yuan, An Electrochemical Biosensor for Sensitive Detection of MicroRNA-155: Combining Target Recycling with Cascade Catalysis for Signal Amplification, ACS Appl. Mater. Inter. 1 (2015) 713-720.

[38] A. Zheng, J. Li, J. Wang, X. Song, G. Chen and H. Yang, Enzyme-free signal amplification in the DNAzyme sensor via target-catalyzed hairpin assembly, Chem. Commun. 25 (2012) 3112-3114.

[39] R.M. Dirks and N.A. Pierce, Triggered amplification by hybridization chain reaction, P. Natl. Acad. Sci. USA 43 (2004) 15275-15278.

[40] Y. Chen, K. Huang and K. Niu, Recent advances in signal amplification strategy based on

oligonucleotide and nanomaterials for microRNA detection-a review, Biosens. Bioelectron. (2018) 612-624.

[41] P. Miao, B. Wang, Z. Yu, J. Zhao and Y. Tang, Ultrasensitive electrochemical detection of microRNA with star trigon structure and endonuclease mediated signal amplification, Biosens. Bioelectron. (2015) 365-370.

[42] X. Huang, X. Qi, F. Boey and H. Zhang, Graphene-based composites, Chem. Soc. Rev. 2 (2012) 666-686.

[43] V. Georgakilas, M. Otyepka, A.B. Bourlinos, V. Chandra, N. Kim, K.C. Kemp, P. Hobza, R. Zboril and K.S. Kim, Functionalization of Graphene: Covalent and Non-Covalent Approaches, Derivatives and Applications, Chem. Rev. 11 (2012) 6156-6214.

[44] J.G. Radich and P.V. Kamat, Making Graphene Holey. Gold-Nanoparticle-Mediated Hydroxyl Radical Attack on Reduced Graphene Oxide, ACS NANO 6 (2013) 5546-5557.

[45] H.A. Becerril, J. Mao, Z. Liu, R.M. Stoltenberg, Z. Bao and Y. Chen, Evaluation of solution-processed reduced graphene oxide films as transparent conductors, ACS NANO 3 (2008) 463-470.

[46] H. Chang, G. Wang, A. Yang, X. Tao, X. Liu, Y. Shen and Z. Zheng, A Transparent, Flexible, Low-Temperature, and Solution-Processible Graphene Composite Electrode, Adv. Funct. Mater. 17 (2010) 2893-2902.

[47] J. Zhou, Y. Zhao, J. Bao, D. Huo, H. Fa, X. Shen and C. Hou, One-step electrodeposition of Au-Pt bimetallic nanoparticles on MoS2 nanoflowers for hydrogen peroxide enzyme-free electrochemical sensor, Electrochim. Acta. (2017) 152-158.

[48] J. Choi, K.R. Love, Y. Gong, T.M. Gierahn and J.C. Love, Immuno-Hybridization Chain Reaction for Enhancing Detection of Individual Cytokine-Secreting Human Peripheral Mononuclear Cells, Anal. Chem. 17 (2011) 6890-6895.

[49] S.O. Kelley, J.K. Barton, N.M. Jackson and M.G. Hill, Electrochemistry of methylene blue bound to a DNA-modified electrode, Bioconjugate. Chem. 1 (1997) 31-37.

[50] A.A. Gorodetsky, M.C. Buzzeo and J.K. Barton, DNA-Mediated Electrochemistry, Bioconjugate. Chem. 12 (2008) 2285-2296.

[51] B. Li, A.D. Ellington and X. Chen, Rational, modular adaptation of enzyme-free DNA circuits to multiple detection methods, Nucleic. Acids. Res. e11016 (2011) .

[52] K. Kerman, D. Ozkan, P. Kara, B. Meric, J.J. Gooding and M. Ozsoz, Voltammetric determination of DNA hybridization using methylene blue and self-assembled alkanethiol monolayer on gold electrodes, Anal. Chim. Acta. PII S0003-2670(02)00308-21 (2002) 39-47.

[53] Y. Guo, Y. Wang, S. Liu, J. Yu, H. Wang, X. Liu and J. Huang, Simultaneous voltammetric determination of E-coli and S-typhimurium based on target recycling amplification using self-assembled hairpin probes on a gold electrode, Microchim. Acta. 3 (2017) 745-752.

[54] P. Yin, H.M.T. Choi, C.R. Calvert and N.A. Pierce, Programming biomolecular self-assembly pathways, Nature. 7176 (2008) 314-318.

[55] H. Zhang, Q. Wang, X. Yang, K. Wang, Q. Li, Z. Li, L. Gao, W. Nie and Y. Zheng, An isothermal electrochemical biosensor for the sensitive detection of microRNA based on a catalytic hairpin assembly and supersandwich amplification, Analyst 2 (2017) 389-396.

[56] S. Song, Z. Liang, J. Zhang, L. Wang, G. Li and C. Fan, Gold-Nanoparticle-Based Multicolor Nanobeacons for Sequence-Specific DNA Analysis, Angew. Chem. Int. Ed. 46 (2009) 8670-8674.

[57] C. Ma, W. Wang, Z. Li, L. Cao and Q. Wang, Simple colorimetric DNA detection based on

hairpin assembly reaction and target-catalytic circuits for signal amplification, Anal. Biochem. 2 (2012) 99-102.

[58] Y. Yuan, G. Liu, Y. Chai and R. Yuan, Electrochemical proximity assay-coupled highly nonenzymatic amplifying strategy for total protein of Nosema bombycis detection, Sens. Actuators B: Chem. (2017) 402-407.

[59] L. Fan, G. Zhao, H. Shi, M. Liu and Z. Li, A highly selective electrochemical impedance spectroscopy-based aptasensor for sensitive detection of acetamiprid, BIOSENS BIOELECTRON (2013) 12-18.

[60] X. Wu, Y. Chai, R. Yuan, Y. Zhuo and Y. Chen, Dual signal amplification strategy for enzyme-free electrochemical detection of microRNAs, Sens. Actuators B: Chem. (2014) 296-302.

Fig. 1 SEM images of PPy (A), PPy–rGO (B) and AuNPs/PPy–rGO (500 nm) (C). (D) EDS element analysis of AuNPs/PPy–rGO composite. PPy was prepared by electrochemical deposition of 0.05 M pyrrole in DBSA for 10 cycles.

Fig. 2 CVs **(A)** and EISs **(B)** of different modified electrodes in 0.1 M PBS containing 5 mM $[Fe(CN)_6]^{3-/4-}$, (a) bare GCE, (b) Au/PPy-rGO/GCE, (c) SH-CP/Au/PPy-rGO/GCE, (d) H1+T+H2/SH-CP/Au/PPy-rGO/GCE, (e) H3+H4/H1+T+H2/SH-CP/Au/PPy-rGO/GCE.

Fig. 3 DPVs of the modified electrodes at different conditions in 0.1 M PBS (pH=7.4): (a) H1/SH-CP/Au/PPy-rGO/GCE, (b) H1+H2/SH-CP/Au/PPy-rGO/GCE, (c) H1+T+H2/SH-CP/Au/PPy-rGO/GCE, (d) H3+H4/H1+T+H2/SH-CP/Au/PPy-rGO/GCE.

Fig. 4 The optimization of experimental parameters. The current responses of the biosensor with different H2 concentration **(A)** and CHA incubation time **(B)** for the detection of 5 nM target miRNA in 0.1 M pH 7.4 PBS; Inset: the corresponding DPV peak currents. Error bars: SD, n=3.

Fig. 5 (A) DPVs for the detection of different concentrations of target microRNA with the proposed method in 0.1 M PBS (pH=7.4) (from a to j: 0 fM, 10 fM, 50 fM, 100 fM, 1 pM, 10 pM, 50 pM, 500 pM, 1 nM, 5 nM). **(B)** The corresponding calibration plots of **(A)**. Error bars: SD, n=3.

Fig.6 Selectivity investigation of the method: (a) blank solution (0 pM target miRNA), (b) 500 pM sRNA, (c) 500 pM nDNA, (d) 500 pM nRNA and (e) 500 pM target miRNA. Inset: the corresponding DPV curves.

Scheme 1 (A) Schematic illustration of electrochemical miRNA biosensor based on enzyme-free signal amplification of CHA and HCR. **(B)** Structures of H1, target, H2, H3 and H4.

Figure 1

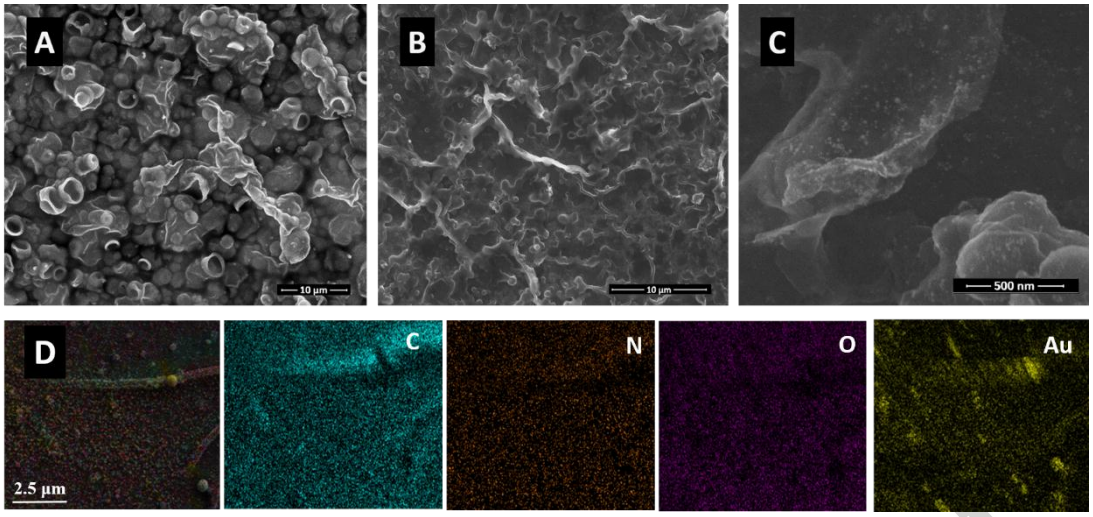

Figure 2

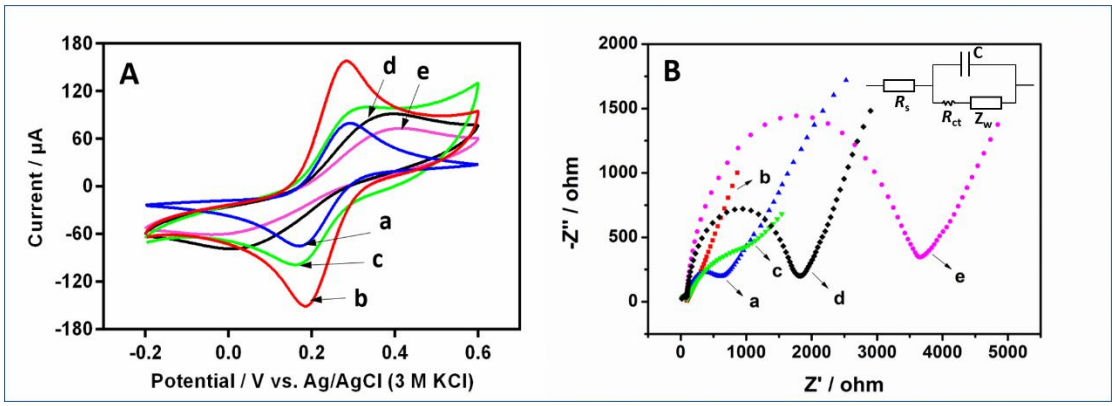

Figure 3

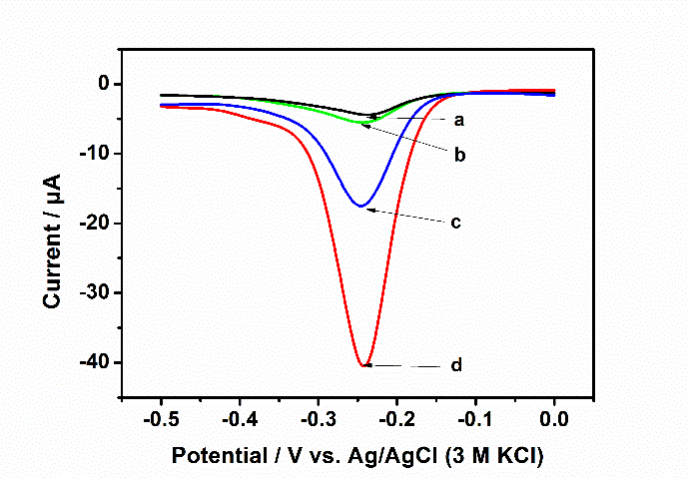

Figure 4

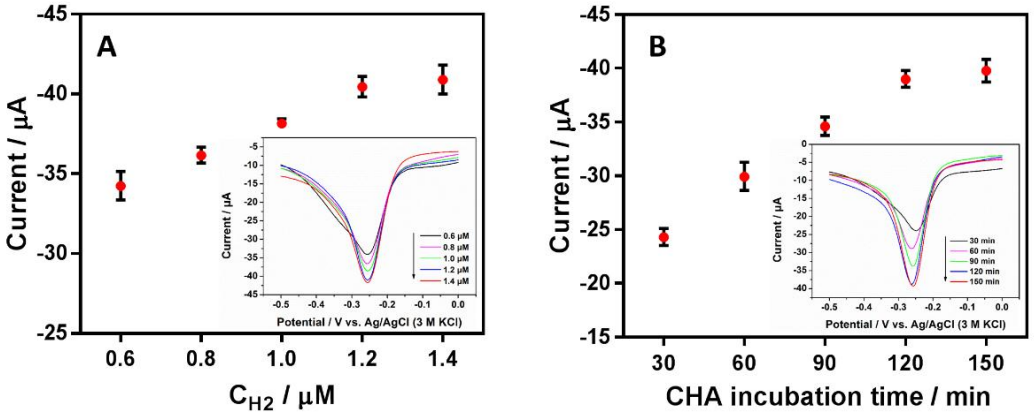

Figure 5

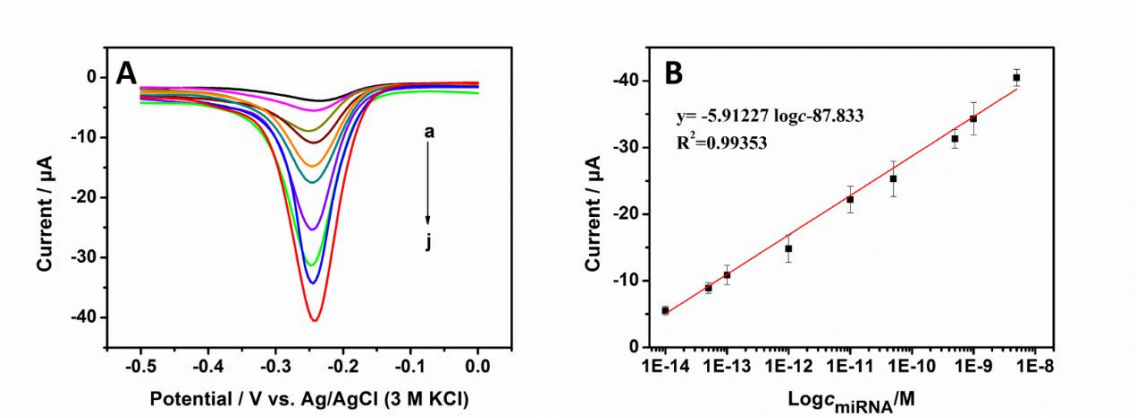

Figure 6

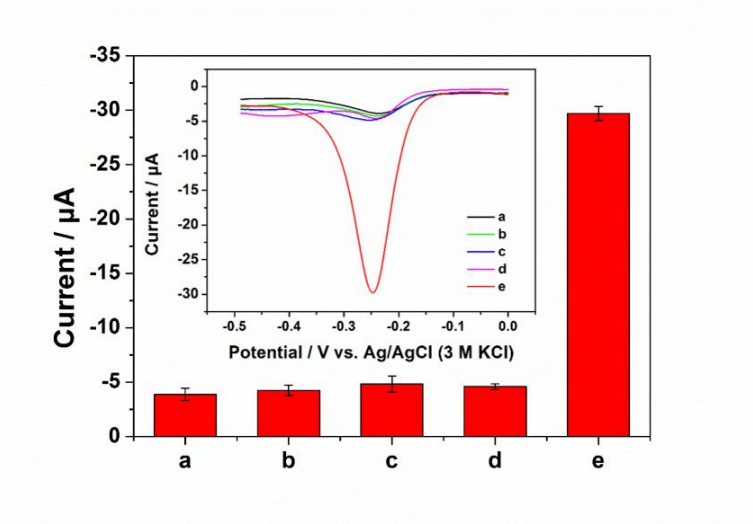

Scheme 1

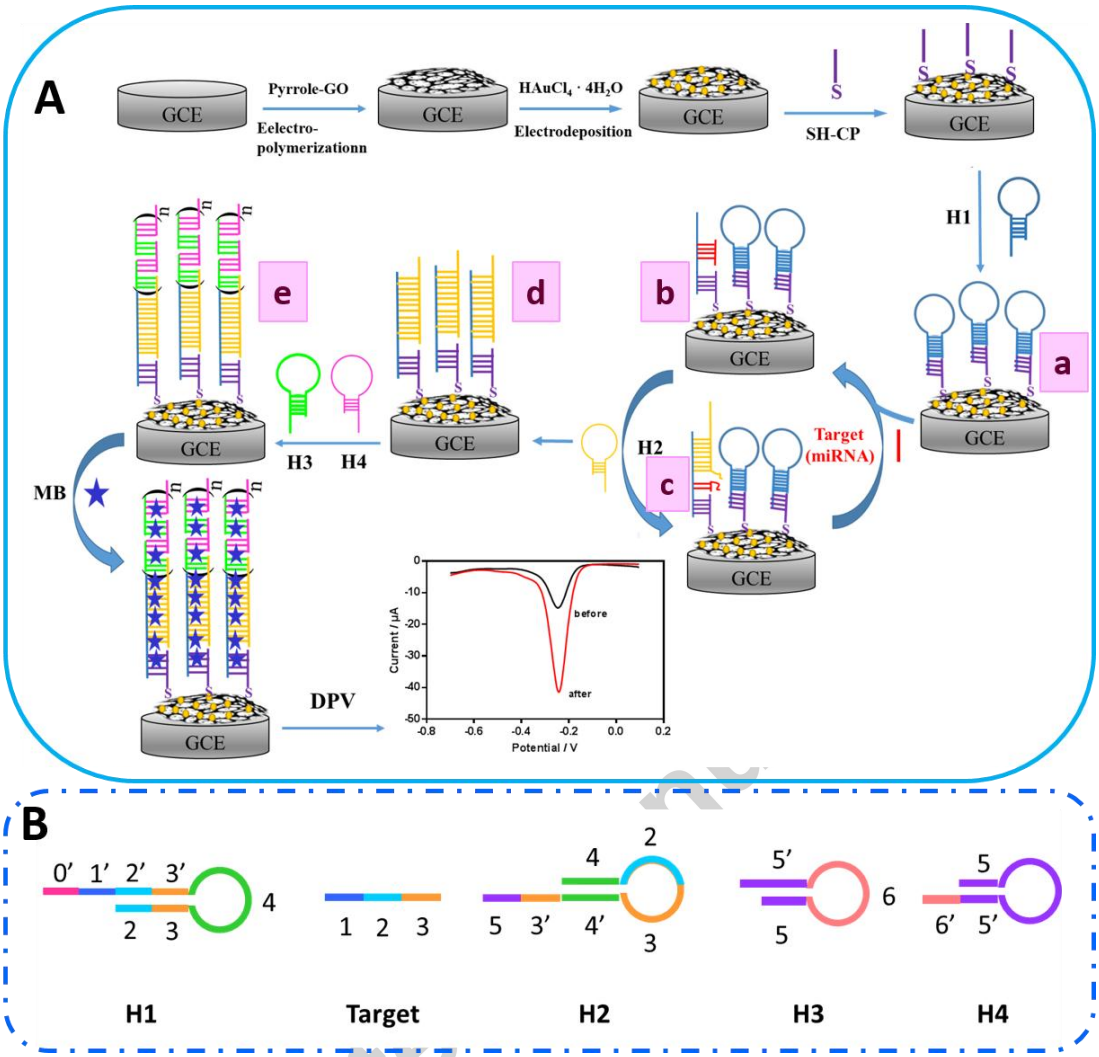

Table 1 All synthesized oligonucleotides used in the experiment[a].

Name	Sequence (5′–3′)
Capture probe (SH-CP)	SH-$(CH_2)_6$-TATTAATCACTCC
miRNA-16（T）	UAGCAGCACGUAAAUAUUGGCG
Hairpin probe (H1)	CGTAAATATTGGCG*AAGGACATGGA*CGCCAATATTTA CGTGCTGCTAGGAGTGATTAATA
Hairpin probe (H2)	AAGGACATGGACGT*AAATATTGG*CGTCCATGTCCTTC GCCAATGAAGAAGCCCCGACT
Hairpin probe (H3)	GCCCCGACT*TGGAACC*AGTCGGGGCTTCTTC
Hairpin probe (H4)	GGTTCCAAGTCGGGGC*GAAGAA*GCCCCGACT
Single-base mismatch (sRNA)	UAGCA**C**CACGUAAAUAUUGGCG
Non-complementary DNA (nDNA)	GGGTTTGGTGGGTTTGGTGG
MiRNA-155 (nRNA)	UUAAUGCUAAUCGUGAUAGGGGU

[a] In the hairpin sequences, loops were italicized and sticky ends were underlined. The bold letter in single-base means mismatch input.

Highlights

- The Au/PPy–rGO nanocomposite was employed as a substrate to immobilize SH-CP and also ensure efficient electron transport of biosensor.
- The combination of CHA and HCR accomplished the target recycling and signal amplification without the assistance of protein enzymes.
- The LOD of the fabricated miRNA biosensor was as low as 1.57 fM.